

# Scaling Invariance in Wave Functions of Quantum Systems on Complex Networks

Huijie Yang<sup>1,\*</sup>, Fangcui Zhao<sup>2</sup>, Yunpeng Wang<sup>1</sup>, and Binghong Wang<sup>1</sup>

<sup>1</sup> *Department of Modern Physics, University of Science and Technology of China, Anhui Hefei 230026, China*

<sup>2</sup> *Life Science and Bioengineering, Beijing University of Technology, Beijing 100022, China*

(Dated: November 20, 2018)

Structure-induced features of the wave functions for the quantum systems on complex networks are discussed in this paper. For a quantum system on a network, the state corresponding to the eigenvalue close to the center of the spectrum is used as the representative state to display the impacts of the structure on the wave functions. We consider the Erdos-Renyi, the WS small world and the growing randomly network (GRN) models. It is found that the probability distribution functions (PDF) of the representative state's components can be described with a power-law with an exponential cutoff in a unified way. For Erdos-Renyi networks, with the increase of the connectivity probability  $p_{ER}$  the PDF turns from power-law-dominated to exponential-dominated functions. For the WS networks in a special region of the rewiring probability  $p_r \in (0, 0.2)$ , where this model can capture the features of real world networks, and the GRN networks, the PDFs obey almost a perfect power-law. These characteristics can be used as the structure measurements of complex networks. They can also provide useful information on dynamical processes on complex networks.

PACS numbers: 89.75.Hc, 72.15.Rn, 05.50.+q, 05.45.Df

The structures of complex networks can induce non-trivial features to the physical processes occurring on them. Typical topics include the epidemic spreading on networks [1, 2, 3], the synchronization of coupling oscillators on networks [4, 5, 6, 7], the response of complex networks to stimuli [8, 9] and so on. In this paper, we consider the impacts of the network structures on the wave functions of quantum systems.

Anderson transition tells us that disorder structures can induce a transition from extended to localized states [10, 11]. Quantum systems with quasi-period structures will be in an intermediate state, which can be described with critical wave functions [12, 13]. The wave function for a localized state decreases exponentially with the distance from its center, while the critical wave function obeys a power-law with respect to the distance. Complex networks have nontrivial structures rather than regular and complete disorder ones. In literature the spectra density function and the time series analysis methods [14, 15, 16] are used to reveal structure-induced features from the spectra [17, 18, 19, 20, 21, 22, 23] and the corresponding eigenvectors [24, 25] of complex networks. In this paper we try to capture the special characteristics of complex networks from the wave functions of the quantum systems on them. These wave functions can provide us useful information on the corresponding classical systems, i.e., the probability distribution function (PDF) of packets walking on the networks at steady states [26]. Consequently, the PDF can shed light on the dynamical processes as the traffic flow [27, 28], the epidemic spreading [1, 2, 3] and the synchronization on networks [4, 5, 6, 7].

We consider an undirected complex network of  $N$  cou-

pling identical oscillators. Denote the adjacent matrix of this network with  $A$ , whose element  $A_{ij}$  is 1 and 0 if the nodes  $i$  and  $j$  are connected and disconnected, respectively. The Hamiltonian of this quantum system reads,

$$\hat{H} = \sum_{n=1}^N \hat{h}_0(x_n, p_n) + \frac{1}{2} \sum_{m \neq n}^N A_{mn} \cdot \hat{V}(x_m, x_n), \quad (1)$$

where  $\hat{h}_0(x_n, p_n)$  is the Hamiltonian of the oscillator  $n$  and  $\hat{V}(x_m, x_n)$  the coupling potential between the oscillators  $m$  and  $n$ . Denote the site energy and the corresponding state of each oscillator with  $\varepsilon_0$  and  $|\varphi_0\rangle$ , respectively. The elements of  $\hat{H}$  read,

$$\begin{aligned} H_{mn} &= \langle \varphi_0(x_m) | \hat{h}_0(x_m, p_m) | \varphi_0(x_n) \rangle \\ &+ A_{mn} \cdot \langle \varphi_0(x_m) | V(x_m, x_n) | \varphi_0(x_n) \rangle \\ &= \varepsilon_0 \cdot \delta_{mn} + A_{mn} \cdot V_{mn} \end{aligned} \quad (2)$$

Assigning  $\varepsilon_0 = 0$  and  $V_{mn} = 1$ , we have  $H = A$ . Hence, the special features of the wave functions of the considered quantum system can be obtained from the eigenvectors of the adjacent matrix  $A$ .

The quantum systems considered in literature have deterministic structures in real world Euclidean space, which lead to nature definitions of the concepts as the localized, intermediate and extended states of the quantum systems. These concepts are also extended to capture the features of quantum systems on small-world networks based on regular lattices, where the long-range edges can be regarded in a certain degree as perturbations to the regular lattices [25]. Obviously, these concepts are invalid for general complex networks without deterministic structures in Euclidean space. Herein, we consider the probability distribution functions (PDF) of the values of the components in the eigenvectors.

\*Electronic address: huijieyangn@eyou.com; Corresponding author

The eigenvector corresponding to the special eigenvalue close to the center of the spectrum for a network, denoted with  $E_c$ , is employed as the representative state to illustrate the features of the considered quantum system. Denote the representative state with  $r = (r_1, r_2, \dots, r_N)$ , where  $r_m$  is the  $m$ th component. Divide the range the probability values of  $\rho = \{N \cdot |r_m|^2, m = 1, 2, 3, \dots, N\}$  distribute into  $M$  bins. Reckon the numbers of the values falling in the bins, respectively. The PDF of the values of the components can be approximated as,

$$P_t \propto K_t \quad (3)$$

where  $K_t$  is the number of the values falling in the  $t$ th bin. The size of the bins can be chosen as a fraction of the variance, i.e.,  $S_{bin} = \frac{1}{J} \cdot \sqrt{\frac{\sum_{m=1}^N \rho_m^2}{N}}$ . In the calculations the parameter  $J$  is assigned 10. It is found that the PDF for different networks can be described with a power-law with an exponential cutoff, which reads,

$$P(T) \propto T^{-\alpha} \exp(-\beta T), \quad (4)$$

$$T = t \cdot (\rho_{\max} - \rho_{\min})/M.$$

For  $\alpha = 0$  and  $\beta = 0$ , the PDF will degenerate to exponential and power-law functions, respectively.

The probability moment (PM) defined as,

$$M_q(E_c) = \sum_{m=1}^N \left( \frac{\rho_m}{N} \right)^q, \quad (5)$$

is also used to measure the global extent of localization. For a perfect extended state we have  $M_q(E_c) = \frac{1}{N^{q-1}}$ , while for a state strongly localized on one node the PM tends to 1. Generally, PM should be in the range of  $[\frac{1}{N^{q-1}}, 1]$ .

As an extreme condition, we consider networks constructed with the Erdos-Renyi (ER) network model. An ER network can be obtained just by connecting each pair of  $N$  nodes with the connectivity probability  $p_{ER}$ . There is a critical point of the connectivity probability  $p_{ER}$ , denoted with  $p_c$ , when  $p_{ER} > p_c$  almost all the nodes tend to form a giant cluster. As shown in figure 1, with the increase of  $p_{ER}$ , the value of the parameter  $\beta$  turns from negative to positive. At the transition point  $p_{ER} = \frac{4}{N} > p_c$ , we have  $\beta = 0.007 \approx 0$ . That is, the PDF is a perfect power-law function. When the connectivity probability  $p_{ER} = \frac{7}{N}$ ,  $\beta$  increases rapidly to 0.31 while  $\alpha$  decreases to 0.87. The PDF is exponential-dominated.

In the WS small-world model the nontrivial features are introduced into the regular lattices just by rewiring with a certain probability  $p_r$  the end of each edge to another randomly selected node. In the rewiring procedure double edges and self-edges are forbidden. In the regular lattices each node is connected with  $d$  right-handed

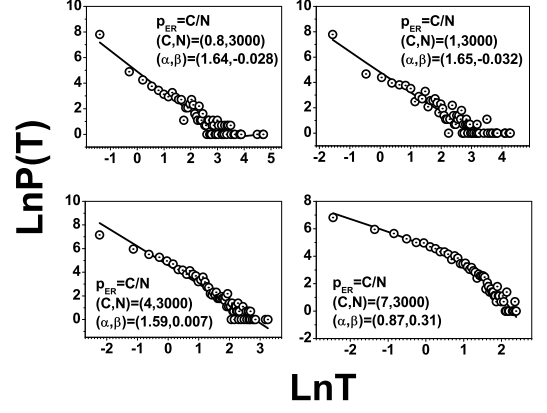


FIG. 1: Typical  $P(T)$  results for the quantum systems on the ER networks. The circles and solid lines are the PDF and the fitting results, respectively. The power-law with an exponential cutoff presented in Eq.(4) can capture the characteristics of  $P(T)$  very well. The value of the parameter  $\beta$  increases from negative to positive. At the transition point  $p_{ER} = \frac{4}{N} > p_c$ , we have  $\beta = 0.007 \approx 0$ , that is, the PDF is a perfect power-law function. When the connectivity probability  $p_{ER} = \frac{7}{N}$ ,  $\beta$  increases rapidly to 0.31 while  $\alpha$  decreases to 0.87. Its PDF tends to be exponential-dominated.

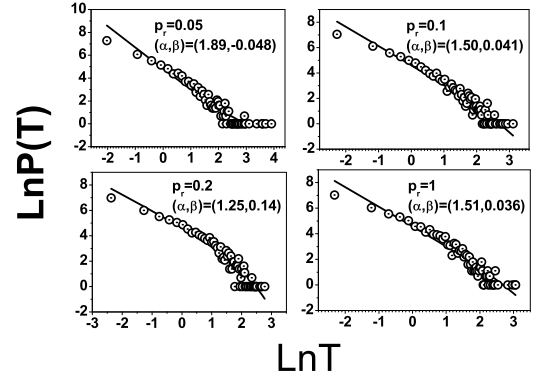


FIG. 2: Typical  $P(T)$  results for the quantum systems on the WS networks. The parameters  $(N, d) = (3000, 2)$ . The circles and solid lines are the PDF and the fitting results, respectively. The power-law with an exponential cutoff presented in Eq.(4) can capture the characteristics of  $P(T)$  very well.

nodes. Figure 2 presents several typical  $P(T)$  results for the quantum systems on the WS networks with different values of rewiring probability. From figure 3 we can find that in the special range of  $p_r \in (0, 0.2)$ , where the model can capture the features of real world networks, the values of  $\beta$  are in the range of  $[-0.06, 0.1]$ , i.e., the PDFs obey almost a perfect power-law. The corresponding values of  $\alpha$  are significant larger than that in the other

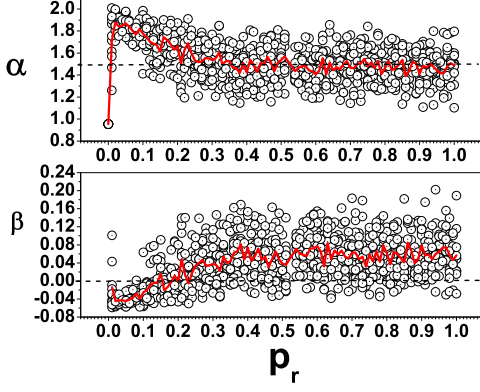


FIG. 3: (Color online) The values of  $(\alpha, \beta)$  for the quantum systems on the constructed WS networks. For each rewiring probability  $p_r$  ten simulated results are presented with open circles, whose averages are shown with the red solid lines.  $(N, d) = (3000, 2)$ . In the interested region of  $p_r \in (0, 0.2)$  the value of  $\beta$  is in the range of  $[-0.06, 0.1]$ . The PDFs obey almost a perfect power-law. The corresponding values of  $\alpha$  are much larger than that in the other regions.

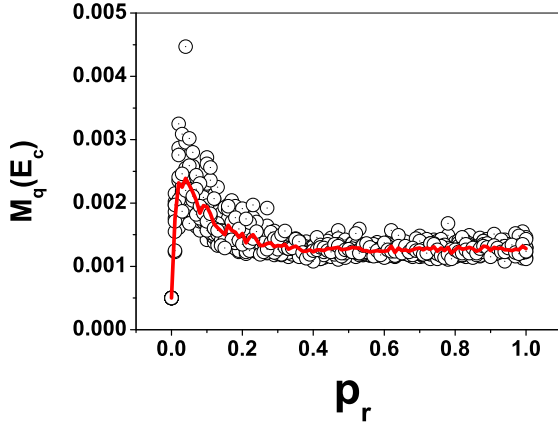


FIG. 4: (Color online) The PM for the quantum systems on the WS networks with different values of rewiring probability. For each rewiring probability  $p_r$  ten simulated results are presented with open circles, whose averages are shown with the red solid lines.  $(N, d) = (3000, 2)$ . In the region  $p_r \in (0, 0.2)$ , the PM values are much larger than that in the other regions. The quantum states on these networks are localized much more than that on the other networks.

regions. Figure 4 presents explicitly the higher extent of global localization of the states for the quantum systems in the region  $p_r \in (0, 0.2)$ . For WS networks with  $d = 5$ , we can obtain similar results.

For the condition  $p_r = 0$ , the constructed WS networks degenerate to one-dimensional regular lattices. The values of  $(\alpha, \beta)$  decrease rapidly to  $(0.96, -1.307)$ . The

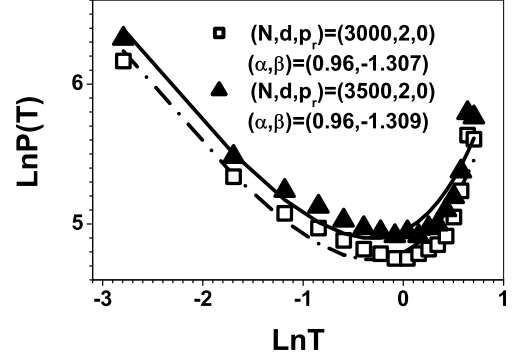


FIG. 5: Typical  $P(T)$  results for quantum systems on the regular lattices. The power-law with an exponential cut-off presented in Eq.(4) can capture the characteristics of  $P(T)$  very well. The values of  $(\alpha, \beta)$  decrease rapidly to  $(0.96, -1.307)$ . The quantum systems on these regular lattices are significantly delocalized compared with that on WS networks (the values of the probability  $\rho$  distribute homogeneously in a much narrower interval). The circles and the solid/dashed lines are the PDFs and the fitting results, respectively.  $(N, d) = (3000, 2)$ .

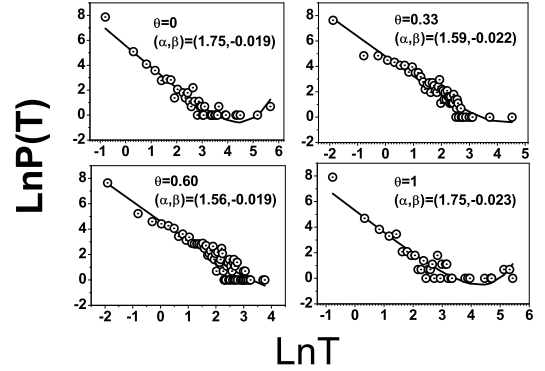


FIG. 6: Typical  $P(T)$  results for the quantum systems on the GRN networks.  $(N, m) = (3000, 1)$ . The circles and solid lines are the PDF and the fitting results, respectively. The power-law with an exponential cutoff presented in Eq.(4) can capture the characteristics of  $P(T)$  very well.

quantum systems on these regular lattices are significantly delocalized compared with that on WS networks (the values of the probability  $\rho$  distribute homogeneously in a much narrower interval).

The growing randomly network (GRN) model simulates a kind of preferential attachment for new added nodes during the growing of the networks. Starting from several connected nodes as a seed, at time  $t + 1$  a new node is linked to  $m$  existing nodes at time  $t$ , denoted as  $\{s_i^t | i = 1, 2, \dots, m\}$ , with the probability

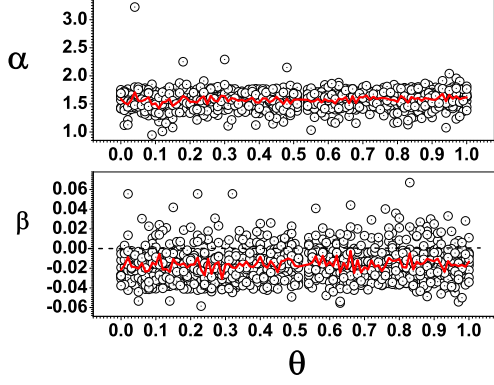


FIG. 7: (Color online) The values of  $(\alpha, \beta)$  for quantum systems on the constructed GRN networks. The values of  $\beta$  are basically in the region of  $[-0.05, 0.05]$ . The PDFs for the quantum systems on these GRN networks obey almost a perfect power-law.  $(N, m) = (3000, 1)$

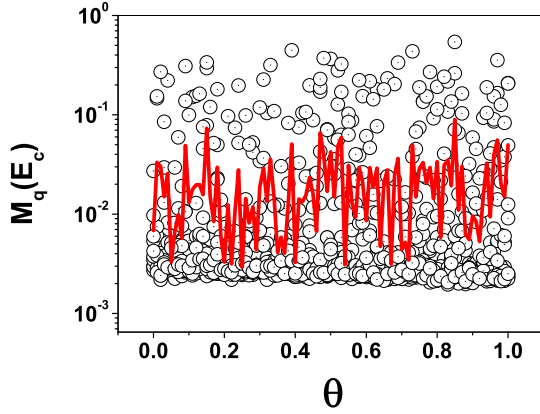


FIG. 8: (Color online) The PM for the quantum systems on the constructed GRN networks. Comparison with the PM results for WS small-world networks shows that the quantum systems on GRN networks are much more localized than that on WS small-world networks.  $(N, m) = (3000, 1)$ .

$p(s_t^i) \propto k(s_t^i)^\theta, 0 \leq \theta \leq 1$ .  $k(s_t^i)$  is the degree of the node  $s_t^i$ .  $\theta = 1$  leads to the BA scale-free model. Several typical results are shown in Figure 6. The values of  $(\alpha, \beta)$  for quantum systems on the constructed GRN networks are shown in figure 7. The values of  $\beta$  are basically in the region of  $[-0.05, 0.05]$ . Consequently, the PDFs for the quantum systems on these GRN networks obey almost a perfect power-law. The global extents of localization are displayed in figure 8.

Figure 9 presents the relation of  $\alpha$  versus  $\beta$ . In this scheme each point corresponds to a network. In the region of  $\beta \approx 0$  the PDF obeys perfect power-law, while a

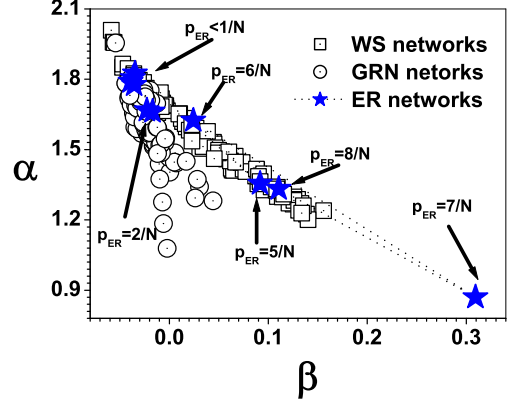


FIG. 9: (Color online) The relation of  $\alpha$  versus  $\beta$ . For same values of  $\beta$ , the  $\alpha$  values for quantum systems on the GRN networks are generally smaller than that on the WS networks. There are much more nodes having large values of  $\rho$  in GRN networks. The ER networks with  $p_{ER}$  less than or near the critical value  $p_c$  ( $p_{ER} \leq \frac{3}{N}$ ) fall into the region of GRN networks, while that with  $p_{ER} \geq \frac{4}{N}$  falls in the region of WS networks. The network with  $p_{ER} = \frac{7}{N}$  falls in the extension of the WS network region. Its large value of  $\beta = 0.31$  tells us that its PDF is exponential-dominated.

significant deviation of  $\beta$  from 0 reveals the exponential-dominated behavior of the PDF. For same values of  $\beta$ , the corresponding  $\alpha$  values for the quantum systems on the GRN networks are generally smaller than that on the WS networks. There are much more nodes having large values of  $\rho$  in GRN networks. This higher extent of localization can be found by comparison the PM values. The ER networks with  $p_{ER}$  less than or near the critical value  $p_c$  ( $p_{ER} \leq \frac{3}{N}$ ) fall into the region of GRN networks, while that with  $p_{ER} \geq \frac{4}{N}$  falls in the region of WS networks. The network with  $p_{ER} = \frac{7}{N}$  falls in the extension of the WS network region. Its large value of  $\beta = 0.31$  tells us that its PDF is exponential-dominated.

In summary, the states of the quantum systems on the WS, GRN and ER networks obey a unified power-law with an exponential cutoff. The WS networks with  $p_r \in (0, 0.2)$ , where the WS model can capture the features of real world networks, and the GRN networks obey almost a perfect power-law. The values of the power-law exponent  $\alpha$  for GRN networks are much smaller than that for the WS networks. With the increase of  $p_{ER}$  the PDF for ER networks tends from almost perfect power-law to exponential-dominated functions. These findings are consistent with the global extent of localizations for the considered networks, which can be displayed explicitly with the PM values.

The two parameters introduced in this paper, denoted with  $\alpha$  and  $\beta$ , are determined by the structures of the considered networks. Consequently, they can be employed as a measurement of the structure characteristics.

The PDF can be used to determine the distribution of traffic packets on networks at steady states. This information may shed light on the dynamical processes on networks, such as the traffic flow, the traffic congestion and the epidemic spreading processes on complex networks.

### Acknowledgements

This work was supported by the National Science

Foundation of China under Grant No.70571074 and No.70471033. It is also supported by the Specialized Research Fund for the Doctoral program of Higher Education (SRFD No. 20020358009). One of the authors (H. Yang) would like to thank Prof. Y. Zhuo and Prof. J. Gu in China Institute of Atomic Energy for stimulating discussions.

- 
- [1] M. E. J. Newman, SIAM Review **45** 117(2003).
  - [2] F. Liljeros, C. R. Edling, L. A. N. Amaral, H. E. Stanley, and Y. Aberg, Nature **411**, 907(2001).
  - [3] H. Yang, F. Zhao, Z. Li, W. Zhang, and Y. Zhou, Int. J. Mod. Phys. B **18**, 2734(2004).
  - [4] M. Barahona, and L. M. Pecora, Phys. Rev. Lett. **89**, 054101(2002).
  - [5] T. Zhou, M. Zhao, and B. Wang, e-print cond-mat/0508368.
  - [6] M. Zhao, T. Zhou, and B. Wang, e-print cond-mat/0507221.
  - [7] S. Jalan, R. E. Amritkar, and C. -K. Hu, e-print nlin.CD/0307037.
  - [8] B. -Y. Yaneer, and I. R. Epstein, Proc. Natl. Acad. Sci. **101**, 4341(2004).
  - [9] F. Li, T. Long, Y. Lu, Q. Ouyang, and C. Tang, Proc. Natl. Acad. Sci. **101**, 4781(2004).
  - [10] P. W. Anderson, Phys. Rev. **181**, 25 (1969)
  - [11] P. A. Lee, and T. V. Ramakerishnan, Rev. Mod. Phys. **57**, 287(1985).
  - [12] C. Tang, and M. Kohmoto, Phys. Rev. B **34**, 2041(1986).
  - [13] M. Kohmoto, B. Sutherland, and C. Tang, Phys. Rev. B **35**, 1020(1987).
  - [14] H. Yang, F. Zhao, W. Zhang, and Z. Li, Physica A **347**, 704(2005).
  - [15] H. Yang, F. Zhao, Y. Zhuo, X. Wu, and Z. Li, Phys. Lett. A **292**, 349(2002).
  - [16] H. Yang, F. Zhao, Y. Zhuo, X. Wu, and Z. Li, Physica A **312**, 23(2002).
  - [17] H. Yang, F. Zhao, L. Qi and, B. Hu, Phys. Rev. E **69**, 066104(2004).
  - [18] F. Zhao, H. Yang, and B. Wang, Phys. Rev. E **72**, 046119(2005).
  - [19] H. Yang, F. Zhao, and B. Wang, e-print cond-mat/0505086. Physica A xxx(2005).(in press).
  - [20] S. N. Dorogovtsev, A. V. Goltsev, J. F. F. Mendes, and A. N. Samukhin, Phys. Rev. E **68**, 046109(2003).
  - [21] I. J. Farkas, I. Deranyi, A. -L. Barabasi, and T. Vicsek, Phys. Rev. E **64**, 026704(2001).
  - [22] R. Berkovits and Y. Avishai, Phys. Rev. B **53**, R16125(1996).
  - [23] M. A. M. de Aguiar and Y. Bar-Yam, Phys. Rev. E **71**, 016106(2005).
  - [24] C. Zhu, S. Xiong, Y. Tian, N. Li, and K. Jiang, Phys. Rev. Lett. **92**, 218702(2004).
  - [25] C. Zhu, and S. Xiong, Phys. Rev. B **63**, 193405 (2001).
  - [26] H. Yang, T. Zhou, W. Wang, B. Wang and F. Zhao, e-print cond-mat:0509354.
  - [27] L. Zhao, Y.-C. Lai, K. Park, and N. Ye, Phys. Rev. E **71**, 026125(2005).
  - [28] A. E. Motter, A. P. S. de Moura, Y.-C. Lai, and P. Dasgupta, Phys. Rev. E **65**, 065102(R) (2002).